DRAFT VERSION MAY 23, 2024
Typeset using LaTeX **twocolumn** style in AASTeX631

Variability of Hundreds of Extragalactic X-ray Binary Systems

TENLEY HUTCHINSON-SMITH,[1,2] ROSANNE DI STEFANO,[2] JULIA BERNDTSSON,[2] DANIEL D'ORAZIO,[2] AND RYAN URQUHART[3]

[1]*Spelman College, 350 Spelman Lane SW, Atlanta, GA 30314, USA*
[2]*Harvard Smithsonian Center for Astorphysics, 60 Garden St., Cambridge, MA 02138, USA*
[3]*ICRAR's Curtin University Node, 1 Turner Ave, Bentley WA 6102, Australia*

ABSTRACT

Planets have not yet been found in X-ray binary (XRB) systems and the characterization of these systems is not yet well understood. One way learn more about XRB systems is to examine their light curves and to identify dips, which could signify a passing planet. This study looks at archived data from the *Chandra X-ray Observatory* in search for interesting time signatures in the light curves of X-ray sources in M51, M101, and M104. Specifically, we present results showing variability in these light curves, which includes dips, flares, and periodicities. We also identify which X-ray sources in our study are located within globular clusters, and we discuss the overall meaning of our results for planet detection as well as for the search for extraterrestrial intelligence (SETI) within globular clusters.

Keywords: X-rays: binaries – galaxies: individual (M51, M101, M104) – globular clusters: general

1. INTRODUCTION

X-ray binaries (XRBs) are systems consisting of a donor star and a compact object, where the compact object accretes matter from the donor star, causing X-rays to be emitted. Some XRBs contain massive donor stars where the accretion is caused by powerful stellar winds, and are referred to as high-mass X-ray binaries (HMXBs). There are also low-mass X-ray binaries (LMXBs), where the donor star is not very massive, and therefore does not have strong enough stellar winds to cause any accretion onto the compact object. Instead, the accretion happens when the star expands to fill its Roche lobe, allowing mass to transfer to the compact object. The compact objects in these systems can either be black holes, neutron stars, or white dwarfs.

X-ray binaries are highly variable, and our goal is to study this variability, which may exhibit itself as flares, periodicities, and dips in the X-ray light curves. Dips could be possible evidence of a passing planet, which is something we are especially interested in finding. Though several planets have been discovered in binary star systems, none have been discovered in XRBs. XRB systems can have planets that orbit either one object in the system (S-type) or both objects in the system (P-type). Planets with S-type orbits are more likely to exist when the XRB has a wide orbit. If the XRB has a relatively small orbit, then planets with P-type orbits are more likely to exist. Many P-type orbits have been observed in non-X-ray binary systems (Butler et al. 1997; Cochran et al. 1997; Roell et al. 2012) (Butler et. al. 1997; Cochran et al. 1997; Roell et al. 2012) as well as S-type orbits (Thorsett et al. 1999; Doyle et al. 2011; Orosz et al. 2012; Hinse et al. 2015). (Thorsett et al. 1999; Doyle et al. 2011; Orosz et al. 2012a, 2012b; Hinse et al. 2015).

Detecting transiting planets in XRBs is easier than detecting transits around other objects or in other wavelengths. This is because the X-ray emitting region is so small, even compared to other planets, that the transiting planet can block out a significant portion of its X-rays, creating a very sharp dip in the light curve.

Several X-ray sources have been discovered in globular clusters, which are large spheroidal aggregations of stars. Globular clusters have a high ratio of X-ray sources relative to the number of stars they contain, and it has been speculated that there is a higher probability for intelligent life to exist in these clusters as well (Di Stefano & Ray 2016) (Di Stefano et al. 2016). This is because interstellar travel to other star systems would be more feasible due to the stars being in close proximity with each other, and a civilization populating multiple star systems would allow long term survival of a given species.

Even though several planets have been detected in binary star systems, none have been discovered in XRB systems. In this study, we used roughly 19 years of archived data from the *Chandra X-ray Observatory* (CXO) to search for interesting time signatures in all the bright sources in the M51, M101, and M104 galaxies. Specifically, we studied the light curves for many hundreds of XRBs, some of which are located in globular clusters, to search for dips, periodicities, and flares. A dip in the light curve may signify a planet, periodicities could be evidence for multiple planets in orbit or signatures

Corresponding author: Tenley Hutchinson-Smith
thutchi3@scmail.spelman.edu

of a close binary, and a flare may be due to an energetic event. It has been hypothesised that X-ray transits are the only way to detect planets in certain systems (Imara & Di Stefano 2018) (Imara et al. 2018), and this study aims to check this hypothesis as well.

The goals of this paper include examining the variabilities in the light curves for each galaxy in this study, while also studying specific variations in the light curves in the form of dips, flares, and periodicities. We then identify which of our sources are located within globular clusters and discuss their variability as well.

2. DATA AND OBSERVATIONS

We are attempting to apply and develop new methods that will allow us to conduct thorough analyses of X-ray light curves. For this preliminary investigation, we chose to work with the light curve data from hundreds of sources from three well observed galaxies: M51, M101, and M104. The light curve data contains time bins that are 3.241 seconds long, with each source having between thousands and tens of thousands of time bins (each source has an observation time of a few kiloseconds to tens of kiloseconds). The number of X-ray photons detected within each time bin is incorporated within our data as well.

2.1. *Sample Selection*

We selected all *Chandra*/ACIS-S and ACIS-I M 51, M 101 and M 104 archival observations with exposure times > 5 ks. We downloaded this data from the public archives and reprocessed them using standard tasks within the Chandra Interactive Analysis of Observations (CIAO) Version 4.9 software package (Fruscione et al. 2006). High particle background intervals were filtered out. The lightcurves of all bright ($L_X \gtrsim 10^{38}$ erg s^{-1} in at least one observation) sources were extracted using circular regions. The size of each region used, per source and observation, was equivalent to the 95% enclosed-counts fraction *Chandra* point spread function (PSF) at the source off-axis position (at an energy of 2 keV). Sources were selected from the Liu 2011 catalog. Lightcurves were created with the CIAO task *dmextract*.

2.2. *Chandra Observations*

The light curves show us how many photons are coming from a given X-ray source per unit time and allow us to study changes in the photon counts. A sudden decrease in the number of photons could signify an object, such as a planet or star, blocking out most or all of the light from the source. It is also possible for an object to be in a very close orbit with the X-ray source, and thus having a transit that only blocks out a small portion of the light, creating a shallow dip in the light curve. Objects with short orbital periods can also be detected by observing periodicities in the light curves, which can represent an object blocking out some or all of the X-ray photons with each revolution it takes. This can be true for a single planet as well as for multiple planets in the system. Additionally, periodicities in the light curve could also constitute a close binary system, where one object in the binary, such as a star, blocks out the X-rays from the accretor periodically. If a given light curve shows a sudden increase in photons, it could be evidence for the end of a transiting object or even the beginning of an energetic X-ray event, such as a flare. Using the extracted light curves, we have studied the count rates and the periodograms of bright X-ray sources as a function of time to search for these kinds of dips, flares, and periodicities.

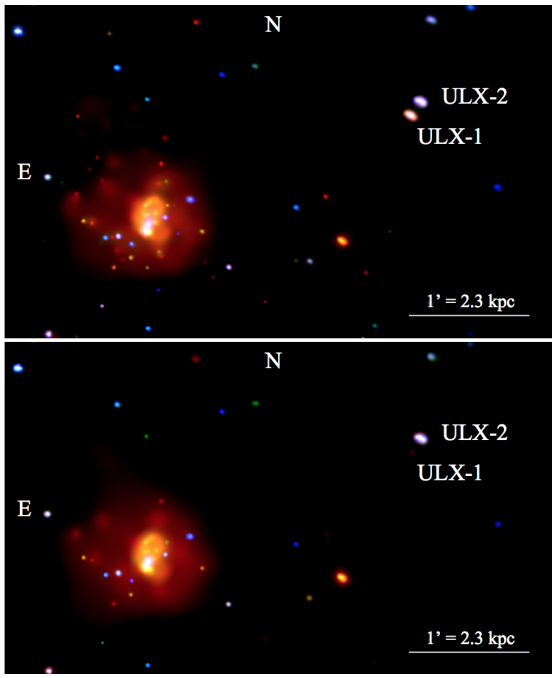

Figure 1. Before (top panel) and after (bottom panel) images of the CXOM51 J132940.0+471237 region in M51 from the 13814 observation, first appearing in Urquhart & Soria (2016). The two X-ray sources are labeled as ULX-1 and ULX-2. Both X-ray sources are visible in the top panel, but in the bottom panel ULX-1 cannot be seen due to an eclipse.

Multiple X-ray eclipses have already been detected from two sources in M51, and what is interesting is that these X-ray sources were discovered within the same region (CXOM51 J132940.0+471237) of M51 as well (Urquhart & Soria 2016) (Urquhart et al. 2016) (see Figure 1). The rarity of such a discovery gives us a reason to speculate that there could be many other eclipsing sources that may have been missed in the CXO archival data set.

In Table 1 we show all the galaxies that were used in this study, along with the observation IDs, exposure times, and the number of X-ray sources corresponding to each observation ID. The length of the exposure time is important for us to consider when trying to detect different phenomena because changes in the light curves can depend on how long it takes an object to pass in front of the X-ray source. If the exposure time is too short, we may not be able to see a dip in the light curve or a be able to find periodicities. The observation IDs corresponding to each galaxy share the same X-ray sources, with an exception of M51 where some X-ray sources only appear in some but not all of its observations.

Table 1. *Chandra* observations used in this study

Galaxy	Obs ID	Exp Time (ks)	X-ray Sources
M51	15553	37.57	56
	15496	40.97	56
	13815	67.18	55
	13816	73.1	56
	13814	189.85	55
	13812	157.46	55
	13813	179.2	55
	12668	9.99	56
	12562	9.63	56
	3932	47.97	56
	1622	26.81	56
	354	14.86	56
M101	14341	49.09	64
	6175	40.66	64
	6170	47.95	64
	6169	29.38	64
	6152	44.09	64
	6118	11.46	64
	6115	35.76	64
	6114	66.2	64
	5340	54.42	64
	5339	14.32	64
	5338	28.57	64
	5337	9.94	64
	5323	42.62	64
	5322	64.7	64
	5309	70.77	64
	5300	52.09	64
	5297	21.69	64
	4737	21.85	64
	4736	77.35	64
	4735	28.78	64
	4734	35.48	64
	4733	24.81	64
	4732	69.79	64
	4731	56.24	64
	934	98.38	64
M104	9553	88.97	119
	9532	84.91	119
	1586	18.51	119

Table 1 *continued*

Table 1 *(continued)*

3. RESULTS

We have observed significant variability in our light curve data. We have examined all the light curves corresponding to each source, and rarely do we see a consistent flow or pattern of X-ray photons, making it so most of the light curves have changing count rates. Unless stated otherwise, all the count rates used in this study are calculated by taking the instantaneous photon count rate from a single time bin, then subtracting the mean count rate from the source's full observation.

It is essential for our analysis to compare different observations of the same source because it allows us to see if the source's variability changes with time. We do this by showing additional count rates for the sources in sections 3.1 and 3.2 during different observation times in the Appendix.

In M51, the highest average count rate is 0.2309 counts per second, and the lowest average count rate is 0.0001 counts per second. In M101, the highest average count rate is 0.287 counts per second and the lowest is 8.9477×10^{-5} counts per second. Lastly, M104's maximum average count rate is 0.43 counts per second, and its lowest is 3.5948×10^{-5} counts per second. We will take a closer look at the count rate variabilities in the following sections.

3.1. *Flares*

We discovered three strong flares in the data set, one in M104, one in M51, and one in M101. Additional count rates for these sources are located in the Appendix (Figures 8 and 9). The flare discovered in M104 came from source J123945.204-113849.99 during the 9533 observation, and contains the highest count rate out of all three flares (Figure 2). The count rate during this observation remained relatively low until 68 ks, where it increases significantly, creating a large spike in the light curve. The maximum count rate of 0.27 counts per second takes place at 71 ks, then decreases afterwards.

The M51 flare is from source J133007.553+471106.00 with observation ID 13812 (Figure 3). Unlike the flare in M104, the count rate for this source starts to increase at the very beginning of the observation, reaches its highest count rate of 0.06 counts per second at 15 ks, and then decreases at approximately 20 ks. What is interesting is that close to 160 ks, the count rate increases again to approximately 0.05 counts per second. Whether the count rate continues to increase after this point is unknown to us since the observation ended at this time.

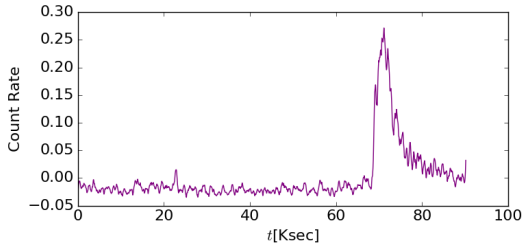

Figure 2. Count rate for source J123945.204-113849.99 in M104 with observation ID 9533. At 68 ks, the count rate significantly increases, reaches its peak at 71 ks, then decreases afterwards. The minimum count rate within this figure is -0.03 counts per second and the maximum count rate is 0.27 counts per second.

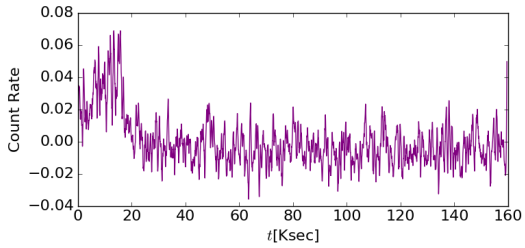

Figure 3. Count rate for source J133007.553+471106.00 with observation ID 13812 in M51. Starting at the beginning of the observation, the count rate increases until it reaches its maximum of 0.06 counts per second at about 15 ks. The minimum count rate is about -0.04 counts per second.

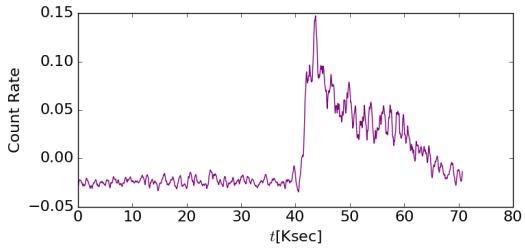

Figure 4. Count rate for source J140229.904+542118.79 in M101 during the 4732 observation. The minimum count rate is -0.03 counts per second at the 40 ks mark. Immediately after, the count rate significantly increases and reaches its maximum of 0.15 counts per second at 44 ks, then steadily decreases until the end of the observation.

The last flare came from source J140229.904+542118.79 during observation 4732 in M101 (Figure 4). The count rate remains relatively low, and reaches its minimum of -0.03 counts per second at 40 ks into the observation. Immediately after it reaches its minimum, the count rate increases considerably and reaches its maximum count rate of 0.15 counts per second at 44 ks. The count rate then gradually decreases for the remainder of the observation.

3.2. *Dips*

We found two dips in the data set, which both correspond to source J132943.306+471134.80 (Figure 5). We also show additional count rates in the Appendix (Figure 9) that show the other observation times for this source. During the 13814 observation, there is a sharp dip in the light curve at 151 ks. Between 27 and 36 ks, there is another, more shallow dip in the light curve. The minimum count rate during this observation is -0.01 counts per second and the maximum count rate is 0.02 counts per second.

For the 13815 observation, there appears to be possible evidence of a dip between the beginning of the observation and 15 ks. We do not know for certain that this is a dip since we cannot study the count rate before the beginning of the observation. The minimum count rate for this observation is -0.01 counts per second and the maximum is 0.02 counts per second. If this is a signature of a dip, then this source is particularly interesting because our observed dips in both observations could be evidence for multiple objects in orbit with the X-ray source.

3.3. *Periodicities*

To identify periodicities in the light curves, we used the Lomb-Scargle periodogram, which is an algorithm that identifies periodic behavior in data sets that may not be obvious to the eye. Specifically, we used the Lomb-Scargle function from the SciPy ecosystem for Python. We made periodograms for the light curves containing at least 2,000 X-ray photons (31 light curves total) as a starting point in our analysis. Out of these 31 periodograms, there are four that contain peaks with relatively high amplitudes. Finding significant peaks in these periodograms tells us that there may be periodic behavior within the light curve with a period taking place every certain number of seconds.

In Figure 6, we show two Lomb-Scargle periodograms and their corresponding count rate plots, both for source J140414.196+542604.52 in M101. For the 4736 observation, there is a peak in the periodogram with an amplitude of 0.36 at 3.9 ks. This could signify a periodicity in the light curve with a period of 3.9 ks. For observation 934, the periodogram shows that there is a period every 3.5 ks in the light curve. The count rate plots for these two observations vary a lot from each other, which may be the reason for the differences in their corresponding periodograms.

We show two more periodograms and their corresponding count rates in Figure 7. The first one is for source J133007.553+471106.00 in M51 with observation ID 13813. There are two significant peaks in this periodogram, one at 0.5 ks and one at 4.6 ks. The second periodgram corresponds to J140515.646+542458.14 in M101 with observation ID 4736. Here, there is a sharp peak at 3.9 ks.

Even though these Lomb-Scargle plots show possible evidence of periodicities within the data, our Lomb-Scargle analysis is only in its preliminary phase, and we do not know for sure that the peaks symbolize periodic behavior since we have not yet folded the data as confirmation.

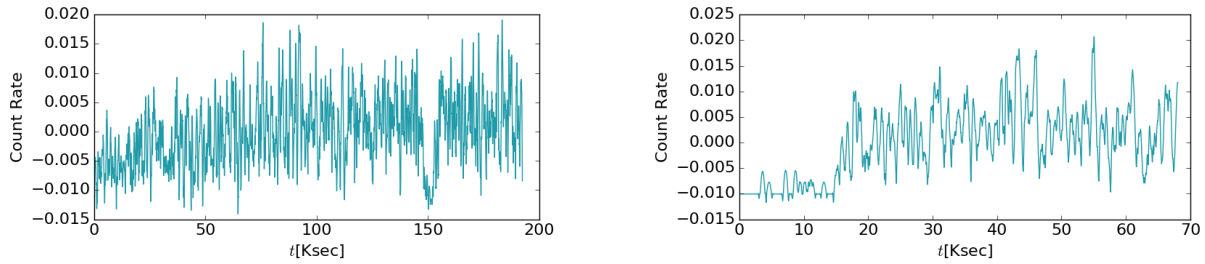

Figure 5. Both of the above plots correspond to source J132943.306+471134.80 in M51. Left: Data comes from observation 13814. There is a sharp dip in the light curve around 150 ks. Specifically, at 147 ks, the count rate decreases until at 151 ks, then starts to increase at 152 ks. Right: This count rate corresponds to observation 13815. The count rate between the beginning of the observation and 15 ks is significantly lower than the count rates for the remaining of the observation.

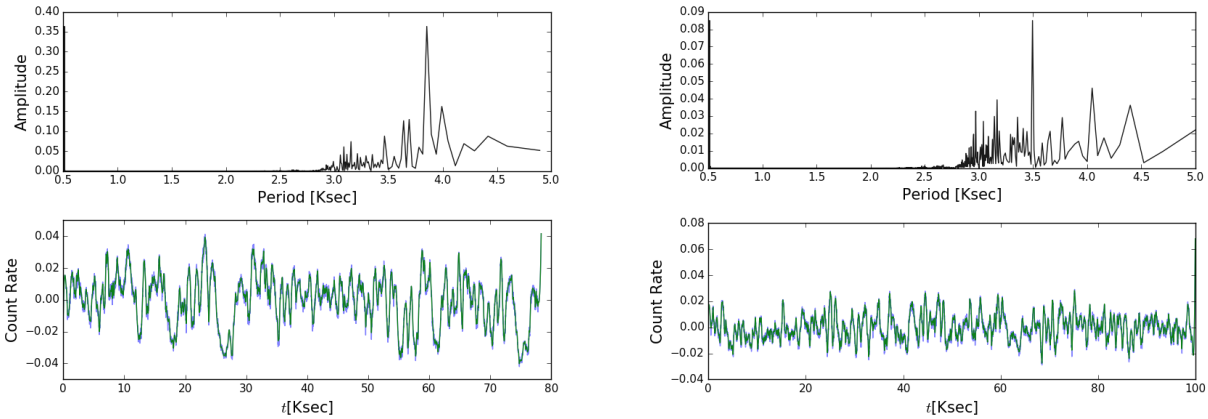

Figure 6. Two Lomb-Scargle periodograms with their corresponding count rate plots for source J140414.196+542604.52 in M101. Left: Periodogram and count rate plot correspond to observation 4736. There is a peak in the periodogram at 3.9 ks with an amplitude of 0.36. Right: Periodogram and count rate plot correspond to observation 934. At 3.5 ks, there is a peak in the periodogram reaching an amplitude of 0.09.

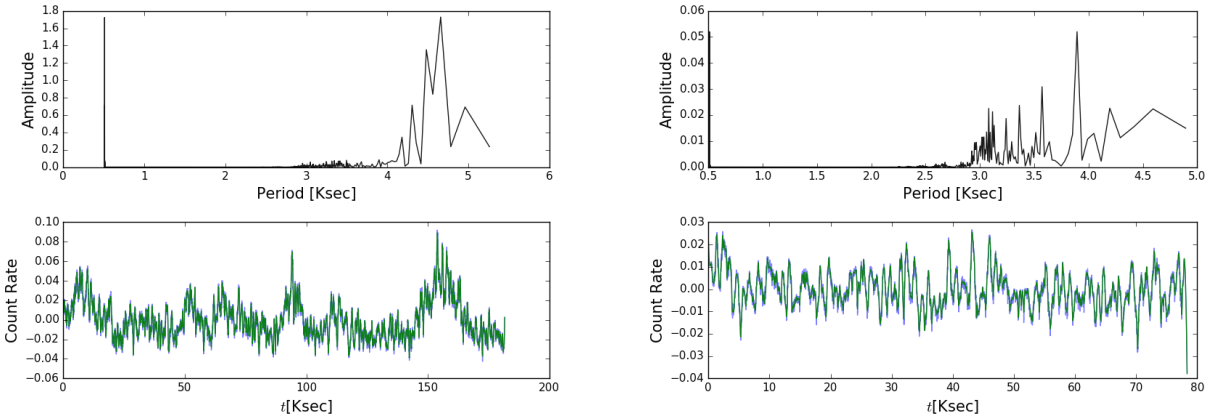

Figure 7. Left: The Lomb-Scargle periodogram and the corresponding photon count rate plot for source J133007.553+471106.00 in M51 with observation ID 13813. The periodogram shows a peak at 0.5 ks with an amplitude of 1.7, as well as a peak at 4.6 ks with an amplitude of 1.7. Right: Periodogram and count rate plot correspond to source J140515.646+542458.14 in M101 with observation ID 4736. A sharp peak with amplitude 0.05 appears at 3.9 ks.

3.4. *X-ray Sources in Globular Clusters*

Several of our X-ray sources are located within globular clusters (see Table 2).

Table 2. Sources in Globular Clusters

Galaxy	X-ray Source
M51	J132952.718+471143.08
M101	J140312.545+542056.26
M104	J123945.559-113933.88
	J123955.795-113449.12
	J123959.261-113828.61
	J123959.772-113455.27
	J124000.660-113520.22
	J123958.656-113728.13
	J123959.069-113720.03
	J123959.410-113727.44
	J124000.324-113723.66
	J124000.701-113704.76
	J124000.914-113702.57
	J124000.960-113708.80
	J124002.179-113721.07
	J124002.743-113717.08
	J124005.652-113711.96
	J124007.001-113753.54
	J123959.424-113723.34
	J123937.721-114031.44
	J123945.245-113601.15
	J123950.935-113823.82
	J123958.877-113655.44
	J123959.664-113525.58
	J124000.934-113654.14
	J124003.617-113242.90
	J124009.686-113645.40
	J124010.397-113639.24
	J123958.769-113725.25
	J124001.258-113702.57
	J123955.418-113849.49
	J123957.338-113750.84
	J123958.951-113838.33
	J123959.009-113512.95

Table 2 *continued*

Table 2 *(continued)*

Galaxy	X-ray Source
	J124003.139-114004.91
	J124005.311-113500.17
	J124008.218-113938.92
	J124012.862-113903.64

We cross-matched all the sources used in this study with other published catalogs containing globular cluster coordinates. For M51, we used the catalog in Harris et al. (2013), and found one source in M51 that is located in a globular cluster (source J132952.718+471143.08). For M101, we again used the Harris et al. (2013) catalog and found that source J140312.545+542056.26 is the only source in M101 located in a globular cluster. In M104, a total of 36 sources were matched with globular clusters from catalogs in the following papers: Bridges et al. (2007), Kundu et al. (2007), Harris et al. (2013), Dowell et al. (2014), Larsen et al. (2001), Spitler et al. (2008), Forbes et al. (2008), Harris et al. (2010), Vazdekis et al. (2010), Misgeld & Hilker (2011), Alves-Brito et al. (2011), Norris et al. (2014).

4. DISCUSSION

4.1. *Flares*

Cataclysmic variables (CVs) are XRB systems consisting of a compact object accreting matter from a close, low-mass companion. Alternatively, XRBs can also be composed of a compact object accreting matter from a giant that is farther away, and these systems are referred to as symbiotics. One of many possible scenarios to explain the observed flares in the light curves would be an XRB system that is in its symbiotic phase (e.g. a black hole with a main sequence star) that then becomes a CV, assuming the main-sequence star was near the end of its lifetime. For this to happen, the original main-sequence star would have turned into a white dwarf, or another kind of compact object, after surpassing its Eddington Limit (the Eddington Limit is the maximum radiation an object can have before the force of radiation overpowers the force of gravity. When a stars radiation exceeds its Eddington limit, its outer layers will escape the star, leaving behind its core). Once the system becomes a CV, the star's leftover core will emit X-rays, creating a light curve flare.

4.2. *Dips*

We found multiple dips in the M51 light curves, which is possible evidence of an object passing in front of the X-ray emitting object. One of the light curve dips observed were relatively shallow, while two were very sharp. Shallow dips may signify an object much smaller than the X-ray object, or located very close to the X-ray object, and thus not being able to block out all the light coming from it. The light curves containing sharp dips would most likely be an indication of

an object that is large enough to block out most, if not all, of the X-rays from the X-ray object.

The dips observed in our light curve data may also be due to an XRB system where one object in the system passes in front of the other, or it can be due to planets with either S-type or P-type orbits within the XRB. Most of the sources in this study are most likely white dwarfs, neutron stars, or accreting black holes, and all of these objects are relatively small compared to planets and main-sequence stars. Due to this, sharp dips in the light curves would most likely be due to either a planet in orbit or a signature of a binary system consisting of the X-ray object and main-sequence star.

4.3. *Periodicities*

Our observed periodicities tell us that either an object has passed in front of the source multiple times, or that multiple objects have passed in front of that source. If the former, the periodic pattern could be due to a planet orbiting the X-ray source. If the X-ray source is part of an XRB system, then P-type and S-type orbits should also be taken into account. For example, the periodicities with longer periods can be a result of a planet with an P-type orbit in the XRB because it would take that planet significantly longer to complete a single revolution. It is also possible that planets with P-type orbits may not show up as periodicities in the light curves if the planet is unable to complete more than one orbit within the given time frame. If this were indeed the case, it may just be perceived as a single dip.

If the light curve periodicity is due to a single planet, it is more likely that the planet has an S-type orbit since it takes less time for planets with S-type orbits to complete a single revolution. Another possible reason for our observed periodicities may just be due to the time signatures of the two objects in the XRB, where each passing of one object in front of the other object results in periodic dips.

4.4. *Sources in Globular Clusters*

Di Stefano & Ray (2016) gives detailed explanations for why globular clusters have a high probability of hosting long term intelligent life. One of these reasons is that globular clusters contain stars that are thousands of times closer to each other compared with the typical distances between stars outside of globular clusters. Because of this, it would be easier for advanced civilizations to travel between star systems. Having the ability to travel to different star systems has multiple benefits, such as allowing the civilization to harness more energy from additional stars after the civilizations host star runs out of energy, and allowing the civilization to populate multiple solar systems, which can create life insurance for the species (e.g. an asteroid hits the species home planet, causing all life to go extinct there, but the species itself does not go extinct due to their presence throughout the cluster).

It has also been shown that there are large regions within globular clusters where stable planetary orbits can exist for long periods of time, while also being in close enough proximity to other stars where intelligent life could potentially travel to (Di Stefano & Ray 2016). Due to these reasons, globular clusters in many different galaxies could, in a sense, be buzzing with intelligent life.

Examining the time signatures from X-ray light curves can be applied to the search for extraterrestial intelligence (SETI) within these globular clusters by identifying anomalies in the light curves that do not appear to be caused by a passing planet or other celestial body (Imara & Di Stefano 2018). Assuming advanced civilizations choose to harness a lot of energy from their host stars, structures such as Dyson spheres may be detected, which is a theoretical structure shaped like a sphere that is placed around a star in order to harness as much energy as possible from it (Dyson 1960). Other structures that are put in orbit around the star to capture its energy may be detected as well. It is important to focus on globular clusters for the SETI not just because of the short travel distances between stars in these regions, but because XRBs are especially abundant within globular clusters and are capable of supplying lots of energy that would be desirable for advanced civilizations.

5. SUMMARY

Using archived *Chandra* data, we have presented the light curves of X-ray sources and XRBs containing significant variability in M51, M101, and M104. We have focused on the variability that corresponds to dips, flares, and periodicities, and have connected these variabilities to possible evidence of orbiting planets and the activity of XRBs. Additionally, the abundance of XRBs in globular clusters can be tied to the SETI, specifically when searching for variabilities in light curves. We discussed how the variabilities that appear to be anomalies are possible evidence for structures built by advanced civilizations, such as Dyson spheres or structures that orbit an X-ray source.

We identified three flares, one from each galaxy: source J133007.553+471106.00 with observation ID 13812 in M51, J140229.904+542118.79 in M101 during the 4732 observation, and J140229.904+542118.79 in M101 during the 4732 observation. Source J132943.306+471134.80 in M51 has one sharp dip and one shallow dip in the 13814 observation, and a possible sharp dip in observation 13815. Using the Lomb-Scargle method, we also found four possible periodicities within the data, two corresponding to source J140414.196+542604.52 in M101, one from source J133007.553+471106.00 in M51, and one from source J140515.646+542458.14 in M101.

6. ACKNOWLEDGEMENTS

The SAO REU program is funded in part by the National Science Foundation REU and Department of Defense ASSURE programs under NSF Grant no. AST-1659473, and by the Smithsonian Institution.

7. APPENDIX

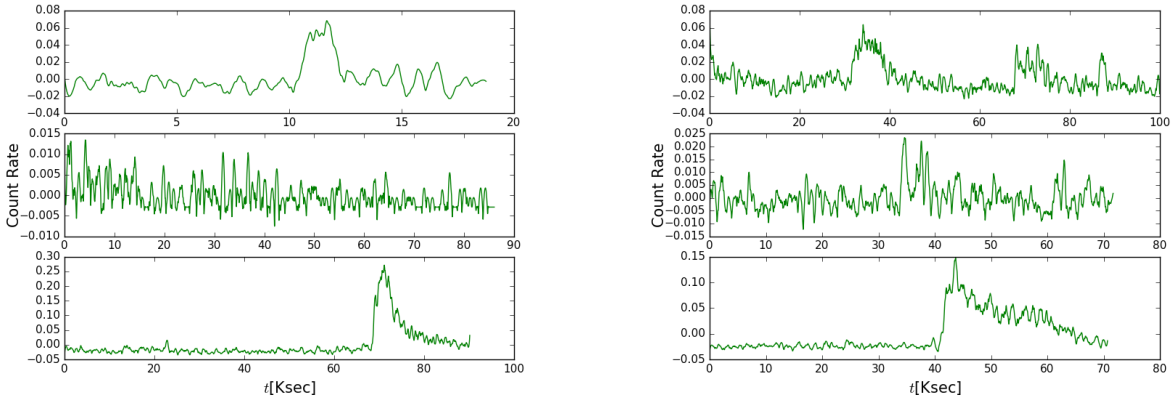

Figure 8. In both plots, the light curves on the bottom are the flares discussed in section 3.1. Left: Source J133007.553+471106.00 in M51 with observation IDs (from top to bottom) 1586, 9532, and 9533. Right: Source J140229.904+542118.79 in M101 with observation IDs (from top to bottom) 934, 5309, and 4732.

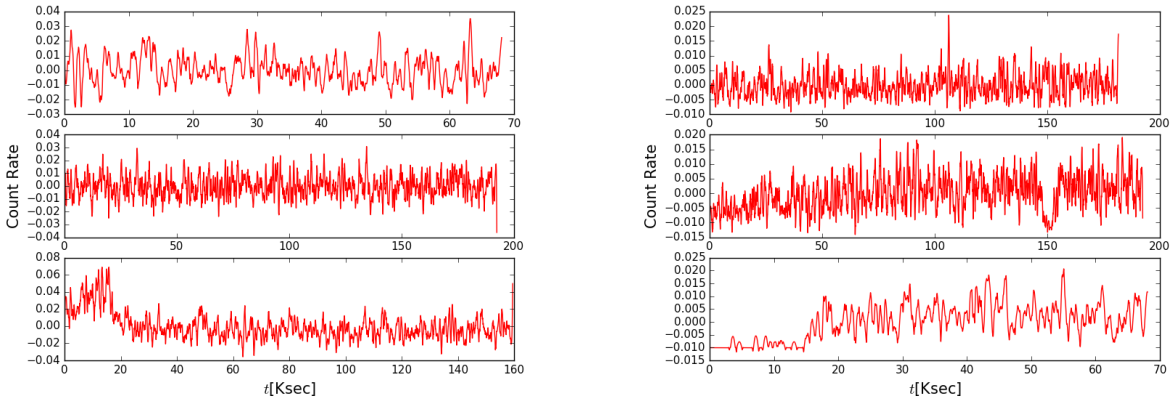

Figure 9. Left: Source J133007.553+471106.00 in M51 with observation IDs (from top to bottom) 13815, 13814, and 13812. The 13812 observation was discussed in section 3.1. Right: Source J132943.306+471134.80 in M101 with observation IDs (from top to bottom) 13813, 13814, and 13815. The bottom two plots were discussed in section 3.2.

REFERENCES

Alves-Brito, A., Hau, G. K. T., Forbes, D. A., et al. 2011, MNRAS, 417, 1823

Bridges, T. J., Rhode, K. L., Zepf, S. E., & Freeman, K. C. 2007, ApJ, 658, 980

Butler, R. P., Marcy, G. W., Williams, E., Hauser, H., & Shirts, P. 1997, ApJL, 474, L115

Cochran, W. D., Hatzes, A. P., Butler, R. P., & Marcy, G. W. 1997, ApJ, 483, 457

Di Stefano, R., & Ray, A. 2016, ApJ, 827, 54

Dowell, J. L., Rhode, K. L., Bridges, T. J., et al. 2014, AJ, 147, 150

Doyle, L. R., Carter, J. A., Fabrycky, D. C., et al. 2011, Science, 333, 1602

Dyson, F. J. 1960, Science, 131, 1667

Forbes, D. A., Lasky, P., Graham, A. W., & Spitler, L. 2008, MNRAS, 389, 1924

Harris, W. E., Harris, G. L. H., & Alessi, M. 2013, ApJ, 772, 82

Harris, W. E., Spitler, L. R., Forbes, D. A., & Bailin, J. 2010, MNRAS, 401, 1965

Hinse, T. C., Haghighipour, N., Kostov, V. B., & Goździewski, K. 2015, ApJ, 799, 88

Imara, N., & Di Stefano, R. 2018, ApJ, 859, 40

Kundu, A., Maccarone, T. J., & Zepf, S. E. 2007, ApJ, 662, 525

Larsen, S. S., Forbes, D. A., & Brodie, J. P. 2001, MNRAS, 327, 1116

Misgeld, I., & Hilker, M. 2011, MNRAS, 414, 3699

Norris, M. A., Kannappan, S. J., Forbes, D. A., et al. 2014, MNRAS, 443, 1151

Orosz, J. A., Welsh, W. F., Carter, J. A., et al. 2012, Science, 337, 1511

Roell, T., Neuhäuser, R., Seifahrt, A., & Mugrauer, M. 2012, A&A, 542, A92

Spitler, L. R., Forbes, D. A., & Beasley, M. A. 2008, MNRAS, 389, 1150

Thorsett, S. E., Arzoumanian, Z., Camilo, F., & Lyne, A. G. 1999, ApJ, 523, 763

Urquhart, R., & Soria, R. 2016, ApJ, 831, 56

Vazdekis, A., Sánchez-Blázquez, P., Falcón-Barroso, J., et al. 2010, MNRAS, 404, 1639